JOC The Journal of Organic Chemistry

Article

pubs.acs.org/joc

Stereochemistry and Solid-State Structure of an Intrinsically Chiral *Meso*-Patterned Porphyrin: Case Study by NMR and Single-Crystal X-ray Diffraction Analysis

Liguo Yang,[†] Yang Zhou,[‡] Mengliang Zhu,[†] Luyang Zhao,[†] Liye Wei,[†] and Yongzhong Bian*[,†]

[†]Beijing Key Laboratory for Science and Application of Functional Molecular and Crystalline Materials, Department of Chemistry, University of Science and Technology Beijing, Beijing 100083, China

[‡]College of Chemistry, Chemical Engineering and Materials Science, Shandong Normal University, Jinan 250014, China

Supporting Information

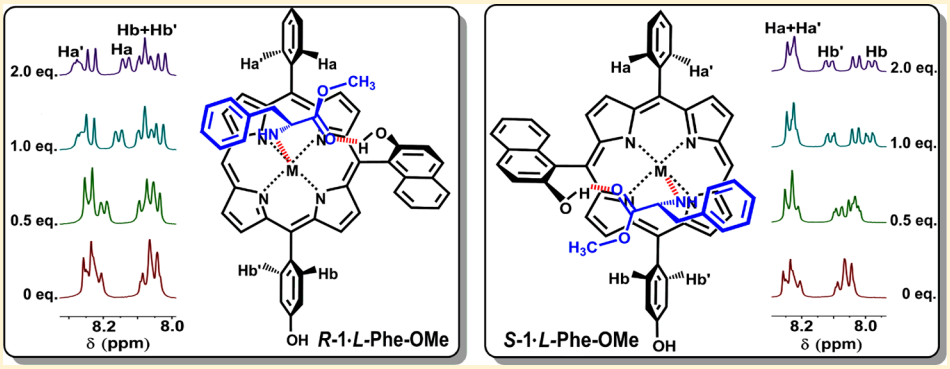

ABSTRACT: A C_1-symmerical *meso*-substituted ABCD-type porphyrin, [5-phenyl-10-(2-hydroxynaphthyl)-15-(4-hydroxyphenyl)porphyrinato]zinc(II) (**1**), has been synthesized and characterized. The molecular structure of **1** has been determined by single-crystal X-ray diffraction analysis. The complex **1** crystallizes in a triclinic system with one pair of enantiomeric molecules per unit cell. Resolution of the racemic mixture has been achieved by chiral HPLC techniques. In particular, the absolute configurations of the enantiomers have been assigned from NMR spectroscopic analysis with L-Phe-OMe as the chiral solvating agent (CSA). The assignments have also been unambiguously confirmed by single-crystal X-ray diffraction analysis. The present results suggest that the CSA–NMR anisotropy strategy is applicable for the stereochemistry determination of chiral host–guest complexes with multiple intermolecular interactions. In addition, the multiple intermolecular interactions between the enantiomerically pure porphyrin *S*-**1** and L-Phe-OMe are proved in the solid state by single-crystal X-ray diffraction analysis.

INTRODUCTION

Chiral porphyrins are of special interest for stereoselective molecular recognition systems,[1] as chiral ligands in asymmetric catalysis,[2] and as chiral optical probes[3] due to their rigid frameworks, versatile substitution at meso/β-positions and coordination with various metals at central cavities, and appropriate spectral and physicochemical properties associated with their large aromatic π-systems.[4] Generally, the chirality of a porphyrin molecule arises from chiral substituents (extrinsic chirality)[5] or by arrangement of achiral substituents along a chiral axis[6] or on a chiral plane[7] to the tetrapyrrole ring (intrinsic chirality). As for the typical example of ABCD-porphyrin possessing four different *meso* substituents (C_s molecular symmetry),[8] the chirality can be generated by breaking of the mirror plane. This can simply be achieved by incorporating a low symmetrical aryl group such as mono-ortho-substituted phenyl or 1-naphthyl at one *meso* site, which introduces a restricted rotation. The resulting atropisomers are of inherent conformational C_1-chirality, Scheme 1.

Scheme 1. Two Atropisomers of ABCD-porphyrin with Restricted Rotation at One of the *Meso* Sites

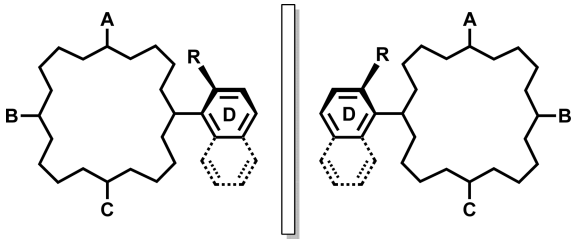

Until now, several *meso*-patterned porphyrins with intrinsic chirality have been developed by researchers. Ogoshi and co-workers reported the synthesis and chiral recognition properties of *trans*-5,15-bis(2-hydroxyphenyl)[9] and *trans*-5,15-bis(2- hydroxynaphthyl)[10,11] substituted pophyrins, and both series have an ABCB-type pattern

Received: August 18, 2013
Published: September 11, 2013

dx.doi.org/10.1021/jo401825k | *J. Org. Chem.* 2013, 78, 9949–9955

and axial chirality with C_2 symmetry. Churchill and co-workers reported a racemic mixture of *meso*-ABC-metallocorrole with planar chirality.[12] It is worth noting that despite the relatively long history of *meso*-substituted ABCD-porphyrins,[13] chiral porphyrin with four distinct *meso*-substituents still remain extremely rare, limited to the two examples of Senge et al.;[14] however, their stereostructures have not been discussed so far. On the other hand, ABCD-porphyrins offer valuable platforms for the designed type and arrangement of different *meso*-substituents to represent cooperative multiple intermolecular interactions, which is important for the molecular recognition and catalytic activity of chiral porphyrins. Thus, we are motivated to develop novel chiral ABCD-porphyrins with a view to create new applications in supramolecular chemistry and catalysis. Herein we report the synthesis of an intrinsic chiral porphyrin with C_1 symmetry, namely [5-phenyl-10-(2-hydroxynaphthyl)-15-(4-hydroxyphenyl)-porphyrinato]zinc(II) (**1**). The enantiomers of **1** were separated successfully, and their absolute stereostructures were assigned on the basis of NMR spectroscopic analysis with an amino acid ester as the chiral solvating agent (CSA). The assignments have been proven in the solid state by single-crystal X-ray diffraction analysis.

RESULT AND DISCUSSION

Design and Synthesis. The two enantiomers of **1** are shown in Figure 1. A 2-hydroxynaphthyl group is introduced at one of the *meso* positions. The large steric hindrance of the 9-hydrogen atom and 2-hydroxy group of the naphthyl ring with the two adjacent porphyrin *β*-hydrogen atoms effectively hinders the free rotation about the naphthyl-*meso* carbon bond,[15] thus prohibiting atropisomerization. In addition, the 2-hydroxy group can serve as a hydrogen bonding donor for guest molecule binding.[15] Another potential binding site is the Zn(II) ion, which is a Lewis acid and can bind Lewis base via coordination bond.[6,16] The other two opposite *meso*-sites are substituted by phenyl and 4-hydroxyphenyl, respectively. The different electron-donating capacities and polarities between these two groups are crucial for the chiral discrimination and resolution properties. The two hydroxyl groups and, in particular, the remaining free *meso*-position allow this porphyrin molecule for further modification and as potential building block for elaborated chiral porphyrin arrays.

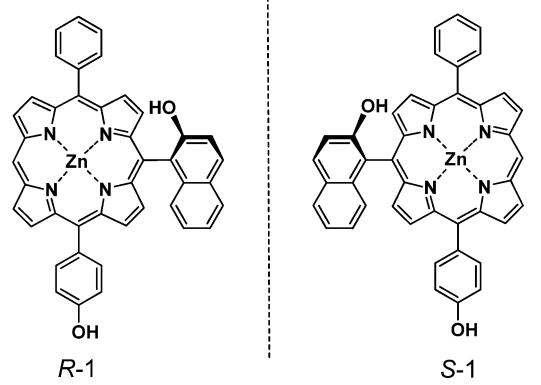

Figure 1. Two enantiomers of **1**, the *R*- and *S*-configurations are defined with Cahn–Ingold–Prelog (CIP) priority rules.

The synthesis of **1** is based on a postmodification approach,[17] as shown in Scheme 2. The *trans*-AB-porphyrin **2** was prepared by a standard [2 + 2] condensation reaction of dipyrromethane and the respective aldehydes.[18] The *n*-hexadecyloxyl group can increase the solubility and facilitates the separation of **2** from its symmetrical byproducts (*trans*-AA- and BB-porphyrins) by gel permeation chromatography (GPC). Then **2** was converted to its zinc complex **3** and subjected to bromination with *N*-bromosuccinimide (NBS). The monobrominated species **4** was isolated and underwent a Suzuki–Miyaura coupling reaction[19] with 2-methoxy-1-naphthylboronic acid. The alkoxy version of a chiral ABCD-porphyrin **5** was hydrolyzed by BBr_3 to convert to the free-base hydroxy version **6**, followed by Zn(II)–metalation to obtain complex **1**. The target compound **1** and the intermediates **2**–**6** were characterized by mass, NMR, and electronic absorption spectroscopies in addition to elemental analysis (see the Experimental Section for details).

Scheme 2. Synthesis of 1[a]

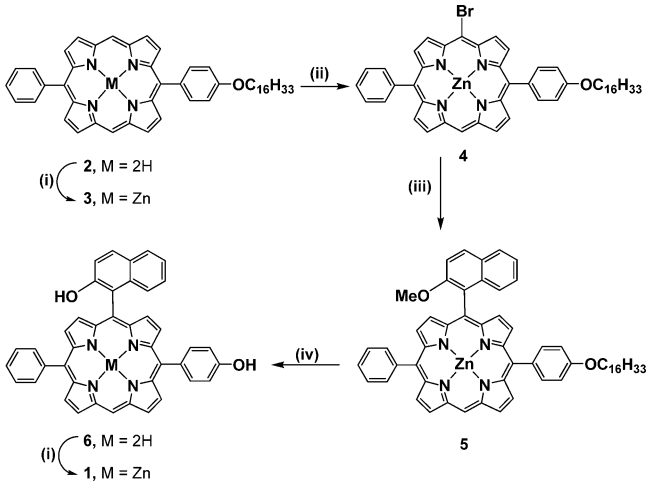

[a]Conditions: (i) $Zn(OAc)_2$, $CHCl_3$/EtOH; (ii) NBS, pyridine, $CHCl_3$/acetone; (iii) 2-methoxy-1-naphthylboronic acid, $Pd(PPh_3)_4$, K_2CO_3, DMF/toluene; (iv) BBr_3, CH_2Cl_2.

Molecular and Crystal Structure of Racemic 1. The molecular structure of **1** was also studied by X-ray diffraction analyses. Suitable crystals of **1** were obtained by slow diffusion of hexane into a solution of **1** in $CHCl_3$/pyridine (100:1 v/v). As shown in Figure 2, the complex **1** crystallizes in triclinic system, nonchiral space group ($P\bar{1}$) with one pair of enantiomeric molecules per unit cell. The Zn center is five-coordinated by four pyrrole nitrogen atoms of porphyrin and one pyridine nitrogen atom, forming a slightly distorted rectangular pyramid coordination geometry. The bond distance of Zn–N(pyridine) (2.139(2) Å) is longer than the mean Zn–N(porphyrin) bond distance (2.073(6) Å), both are similar to the corresponding reported values for other pyridine–Zn–porphyrin systems.[20] Because of the axial coordination of pyridine ligand, the Zn center deviates from the N_4 mean plane (0.323 Å) and points to the axial pyridine ligand. As expected, the naphthyl ring is almost perpendicular to the N_4 mean plane of porphyrin with a dihedral angle of 82.86°, indicating highly restricted rotational freedom of the 2-hydroxynaphthyl group due to the large steric hindrance effects. Notably, another pyridine molecule also binds to the porphyrin host via hydrogen bonding of N(pyridine)---HO(2-hydroxynaphthyl), and the pyridine ring is almost parallel to the porphyrin ring, with a inter-ring distance of 3.290 Å, suggesting some contribution of $\pi-\pi$ stacking for this host–guest binding. Furthermore, a one-dimesional (1D) supramolecular double-chain structure can be observed in the crystal of **1**, the linkages include: (1) hydrogen bondings of O(2-hydroxynaphthyl)---HO(4-hydroxyphenyl) and N(pyridine)---HO(2-hydroxynaphthyl), with distances of 1.900(6) and 1.971(6) Å, respectively. Here,

dx.doi.org/10.1021/jo401825k | J. Org. Chem. 2013, 78, 9949–9955

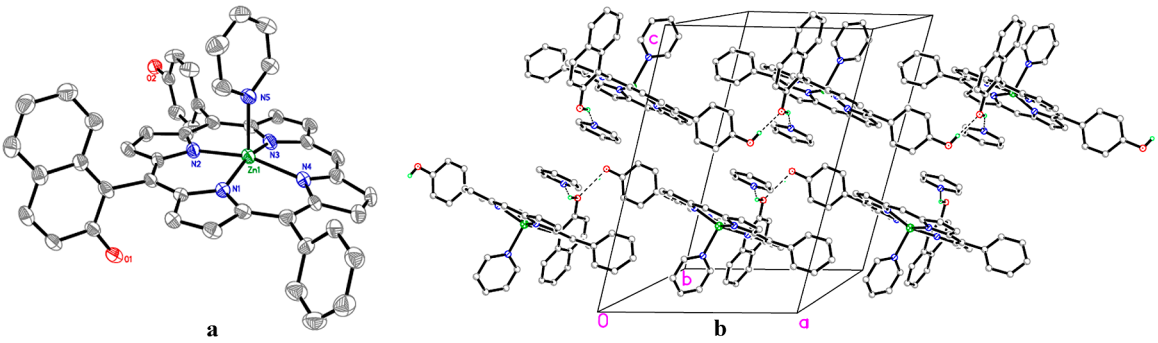

Figure 2. (a) X-ray crystal structure of complex **1** showing the 50% probability thermal ellipsoids for all non-hydrogen atoms. (b) Unit cell of complex **1** shows one pair of enantiomers and 1D double-chain structure. Hydrogen atoms are omitted for clarity.

the hydroxyl of naphthyl serves as hydrogen bonding donor and acceptor both. (2) $\pi-\pi$ stacking interactions of pyridine–porphyrin and pyridine–pyridine, with inter-ring distances of 3.290 and 4.043 Å, respectively. The above observations imply that the porphyrin **1** can be a chiral receptor with multiple binding sites and multiform intermolecular interactions.[21]

Resolution. Attempts to resolve the alkoxy version of the chiral ABCD-porphyrin (**5**) have so far failed even with various chiral HPLC conditions, probably due to the low polarity and the lack of hydrogen-bonding donor of this compound. However, the hydroxy version **1** has been separated into two fractions with a 1:1 ratio by using a chiral HPLC method, as shown in Figure 3.

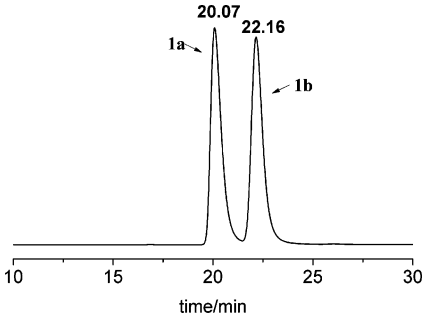

Figure 3. Chromatogram of **1** monitored by a UV detector at 410 nm (i.d. 10 × 250 mm column; 25 °C; 2-propanol/CH_2Cl_2/hexane (1/50/50, v/v/v); isocratic flow rate: 2 mL/min).

The two fractions with retention times of 20.07 and 22.16 min are denoted as **1a** and **1b**, respectively, which show very weak circular dichroism (CD) signals,[9] whereas they possess identical electronic absorption and NMR spectra, indicating the successful resolution of enantiomers.

UV–vis Spectrophotometric Titration. To examine the supramolecular binding capability of the enantiomers **1a** and **1b**, UV–vis spectrophotometric titrations with a pair of amino acid esters (L- and D-Phe-OMe) as the guests were performed at 293 K in $CHCl_3$, Figures 4a and S1a (Supporting Information). Upon adding L- and D-Phe-OMe to **1b** gradually, their Soret absorptions underwent bathochromic shift from 415 to 425 nm due to the formation of complexes **1b**·L-Phe-OMe and **1b**·D-Phe-OMe, respectively. Sharp isosbestic point appears at 420 nm for each titration, which verifies the 1:1 stoichiometry of host to guest and allows determining the association constants (K_{assoc}) by applying a nonlinear curve-fitting method.[22] The K_{assoc} are evaluated as high as 2.3×10^4 and 1.4×10^4 M^{-1} for **1b**·L-Phe-OMe and **1b**·D-Phe-OMe, respectively (errors estimated as ±5%), however, resulting very weak enantioselectivity of 1.6 ($K_{assoc(\mathbf{1b}\cdot\text{L-Phe-OMe})}/K_{assoc(\mathbf{1b}\cdot\text{D-Phe-OMe})}$).

Absolute Configuration Assignment by NMR Analysis. The chiral discrimination interactions of the enantiomers of **1** with L- and D-Phe-OMe were investigated by ^{1}H NMR spectroscopy. Upon mixing **1a** (or **1b**) with L- or D-Phe-OMe in a 1:1 ratio, the NMR signals of the individual host and guest disappeared completely, and the signals of the supramolecular complexes appeared instead as a result of the relatively strong binding affinity, Figure S2 (Supporting Information). These spectra show clear enantiomer/diastereoisomer relations as shown in Figure S3 (Supporting Information). Generally, the NMR signals of L/D-Phe-OMe markedly shifted upfield due to the strong shielding effect of porphyrin ring current,[23] whereas most of those of the porphyrin host were only slightly perturbed by the guest molecule and became well resolved as a result of the loss of motion freedom induced by the host–guest binding. With the exception of the hydroxyl proton of the 2-hydroxynaphthyl group, whose resonances undergo profoundly large downfield shifts from 5.20 to 6.29 ppm for **1a**·L-Phe-OMe and **1b**·L-Phe-OMe both. This is believed to be due to the formation of OH---O=C hydrogen bonding with the guest carbonyl group.[9] By taking the above X-ray diffraction analysis results into account, a two-point fixation binding mode can be reasonably proposed as shown in Figure 5, which is connected by Zn---NH_2 coordination and OH---O=C hydrogen-bonding interactions. The binding mode is similar with previous report,[9] and is also supported by the preliminary density functional theory (DFT) calculation results,[24] as shown in Figures S4 and S5 (Supporting Information). The optimized supramolecular structures are consistent with the proposed one.

As mentioned above, the CD signals of the enantiomers **1a** and **1b** are undetectable; this is also the case after the formation of host–guest complexes with L-Phe-OMe. Thus, their absolute configuration cannot be deduced through chiroptical protocol.[1] On the other hand, because of the anisotropic shielding effects of chiral guest molecules, the complexation-induced shifts (CISs) for the ^{1}H NMR signals of chiral host molecules are diagnostic for their configurational correlations.[25] Particularly in the present case, due to the two-point fixation of the guest with the host, L-Phe-OMe is located at certain positions over the porphyrin plane. Thus, the intensity of the shielding effects for each porphyrin proton is dependent on the distance and relative orientation to a specific group of L-Phe-OMe. As depicted in Figure 5, the binding mode suggests that the pyrrole (I) protons (H1 and H2) should receive relatively strong shielding effects from the benzyl group of L-Phe-OMe and the pyrrole (II) and pyrrole (II′) protons (H3, H3′, H4 and H4′) should be shielded by the ester

dx.doi.org/10.1021/jo401825k | J. Org. Chem. 2013, 78, 9949–9955

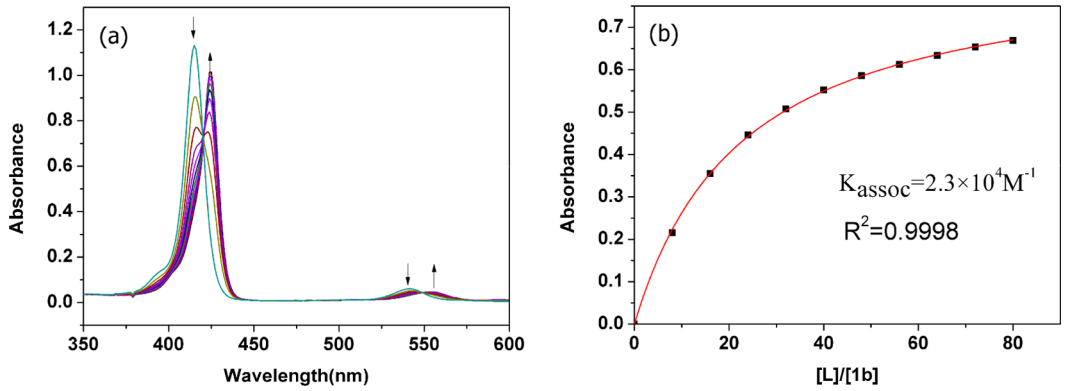

Figure 4. (a) Spectral change upon titration of **1b** with L-Phe-OMe in $CHCl_3$ at 25 °C. (b) Changes in ΔAbs at 415 nm for evaluating K_{assoc}. [**1b**] = 2.0×10^{-6} M; [**L**]/[**1b**] = 0–80.

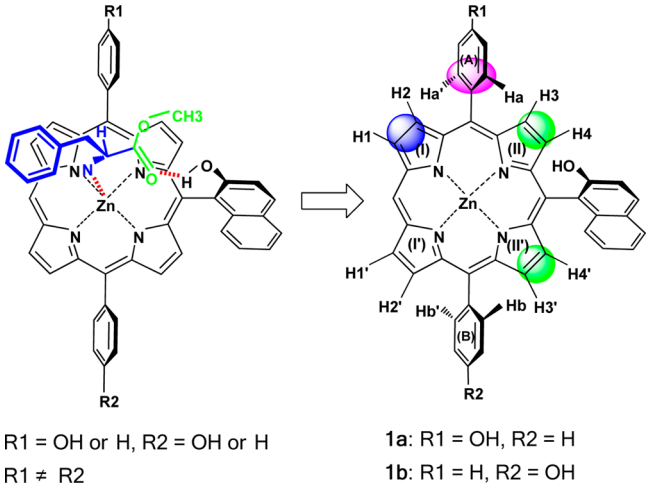

Figure 5. Two-point fixation binding and configurational correlation model of **1**·L-Phe-OMe.

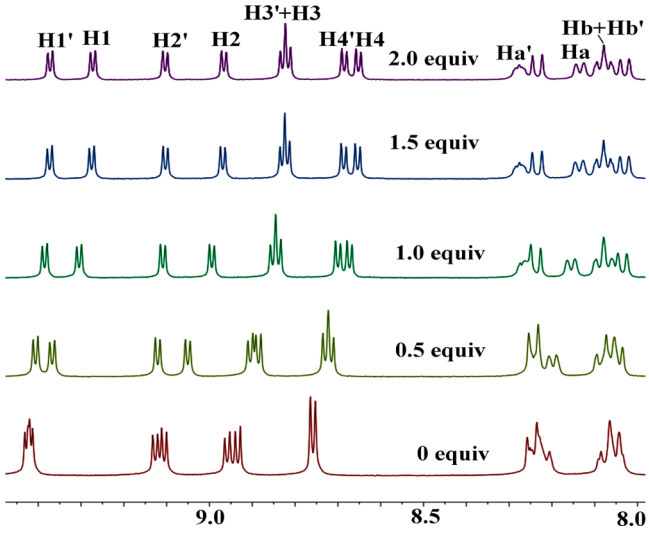

Figure 6. Partial ^{1}H NMR titration spectra of **1b** with L-Phe-OMe (0.5 equiv additions) at 293 K in $CDCl_3$.

(methoxyl) group similarly,[26] whereas the pyrrole (I′) protons (H1′ and H2′) should be less disturbed than other *β*-protons due to the long distances to the guest molecule. Most importantly, one of the two *meso*-aryl groups (A) should be alternatively contiguous to the guest molecule, while the other one should be far from the guest molecule. Thus, the different CISs between *ortho*-protons (Ha, Ha′ and Hb, Hb′) are directly informative for discriminating A and B *meso*-aryl groups in the configurational correlation model.

As expected, clear anisotropic CISs have been observed through ^{1}H NMR titration experiments as shown in Figures 6, S8, and S9 (Supporting Information). Upon addition of 0.5 equiv of guest, the signals of free host disappeared completely, indicating the quick exchange equilibrium compared to the NMR time scale. Gradual addition of guest induced regular shifts of the signals of complexed host until 2.0 equiv of guest was added. The CIS values for selected protons of the porphyrin hosts are listed in Table 1. For example, upon titration of **1b** with L-Phe-OMe, the resonances of H1 and H2 moved upfield by 0.14–0.15 ppm due to the diamagnetic effect of the phenyl ring of L-Phe-OMe, while those of H1′ and H2′ only took place 0.03–0.06 ppm upfield shifts. The NMR signals of the other *β*-protons (H3, H3′, H4, and H4′) also shifted upfield with CIS values of −0.08 to −0.15 ppm. By closely examining the titration profiles in Figure 6, a fine but substantial splitting of the resonance signals for specific phenyl *ortho*-protons Ha and Ha′ were observed, with CISs of −0.09 and 0.04 ppm, respectively. The former is oriented toward the binding side of porphyrin plane, thus experiencing prominent shielding effects from the guest. The latter points to the vacant side, which seems to be dominated by the

Table 1. ^{1}H NMR Complexation-Induced Shifts (CIS, Δ*δ*/ppm) of 1a and 1b upon Addition of 2.0 equiv of L-Phe-OMe in $CDCl_3$ at 293 K[a]

protons		Δ*δ*/ppm[b] 1b	1a
meso-H		−0.26	−0.26
β-H	H1	−0.15	−0.15
	H2	−0.12	−0.14
	H1′	−0.06	−0.06
	H2′	−0.07	−0.03
	H3	−0.11	−0.15
	H4	−0.10	−0.11
	H3′	−0.13	−0.11
	H4′	−0.09	−0.08
phenyl-H	Ha	−0.04	−0.09
	Ha′	0.04	0.04
	Hb and Hb′[c]	0.02	0.01

[a]Signal assignments were made with the help of ^{1}H–^{1}H COSY spectra (Figures S8 and S9, Supporting Information). [b]$\Delta\delta = \delta_{bonded\ host} - \delta_{free\ host}$. [c]Unresolved signals.

dx.doi.org/10.1021/jo401825k | J. Org. Chem. 2013, 78, 9949–9955

deshielding effect of the porphyrin ring. The NMR resolution of Ha and Ha′ also suggests the restricted rotation along the phenyl-*meso* carbon bond, which is induced by the enhanced steric hindrance as a result of the close guest binding. On the contrary, the signals for the other pair of phenyl *ortho*-protons Hb and Hb′ are hardly influenced by complexation, with quite small CIS value (0.01 ppm), and the two protons cannot be distinguished from each other; however, this observation is in conformity with the configurational correlation model in Figure 5, which assumes Hb and Hb′ are away from the shielding area of the guest. On the basis of the above discussion, A and B groups can be rationally assigned to phenyl and 4-hydroxyphenyl, respectively, for **1b**, which corresponds to the *R*-configuration. Similar analysis has been conducted for **1a** and the L-Phe-OMe system, in which A and B groups are assigned to 4-hydroxyphenyl and phenyl, respectively, leading to the *S*-configuration.

2D NOESY measurements provide additional experimental evidence for establishing the configurational correlations. ^{1}H−^{1}H NOESY spectra of **1a**·L-Phe-OMe and **1b**·L-Phe-OMe are shown in Figures S10 and S11 (Supporting Information). Strong nuclear Overhauser effect (NOE) interactions can be observed between phenyl *ortho*-protons (Ha and Ha′) and pyrrole protons (H2 and H3), indicating a close proximity between the mentioned pyrrole protons with the phenyl protons. This is also true for the other set of phenyl *ortho*-protons (Hb and Hb′) and pyrrole protons (H2′ and H3′). The observation is in agreement with the above CIS analysis.

Stereostructure and Multiple Intermolecular Interactions in the Solid State. The effort to prepare single crystals from the pure enantiomers **1a** and **1b** was unsuccessful due to their poor crystallinities. Fortunately, after the formation of a host−guest complex with L-Phe-OMe, suitable crystals of **1a**·L-Phe-OMe for X-ray analysis were obtained by slow diffusion of hexane into a chloroform solution. The absolute structure of **1a**·L-Phe-OMe in the solid state was demonstrated by the single-crystal X-ray analysis results (Figure 7 and Table S1 in the Supporting Information), in

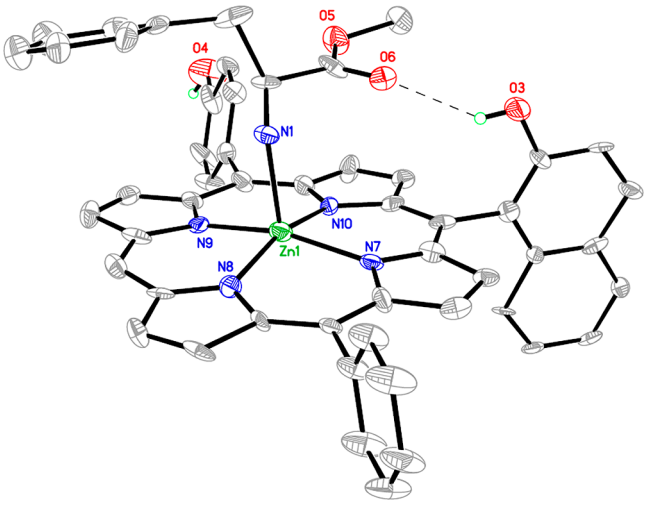

Figure 7. X-ray crystal structure of complex **1a**·L-Phe-OMe. The thermal ellipsoids are scaled to be the 50% probability level.

which the **1a** fraction possesses *S*-configuration, thus confirming the above assignment by NMR analysis.

The complex **1a**·L-Phe-OMe crystallizes in the monoclinic system in a chiral space group ($P2_1$) with four molecules per unit cell. As shown in Figure 7, L-Phe-OMe binds **1a** by Zn---NH_2 coordination (2.151(10) Å) and OH---O═C hydrogen bonding (2.163(14) Å) interactions. The Zn(II) ion is also five-coordinated, forming slightly distorted rectangular pyramid coordination geometry. The Zn center deviates from the N_4 mean plane (0.278 Å) and points to the L-Phe-OMe side. The bond distance of Zn−N(Phe) (2.151(10) Å) in **1a**·L-Phe-OMe is longer than that of Zn−N(Py) (2.139(2) Å) in **1**·2Py, indicating a weakened coordination interaction in the former. The naphthyl ring is almost vertical to the N_4 mean plane of **1a** (84.59°), which is in favor of the formation of OH---O═C hydrogen bond with carbonyl moiety of L-Phe-OMe. In addition, the dihedral angle between the phenyl ring of L-Phe-OMe and the closest pyrrol ring of **1a** is 15.50°, with an interplane distance of 4.024 Å, suggesting weak $\pi-\pi$ interaction in this supramolecular complex.

CONCLUSION

In summary, an intrinsic chiral ABCD-type porphyrin **1** has been synthesized and resolved successfully. The single-crystal structure of the racemic mixture of **1** was obtained by X-ray diffraction analysis. The supramolecular binding of the enantiomers with L- and D-Phe-OMe has been investigated by electronic absorption and NMR spectroscopies, which is believed to be due to the two-point fixation with coordination and H-bonding interactions. The tight two-point host−guest binding allows the establishment of configurational correlations between the amino acid ester guest (L- or D-Phe-OMe) and the porphyrin host (**1a** or **1b**) by analyzing the CIS values of ^{1}H NMR spectroscopy. Notably, here the amino acid ester serves as a chiral solvating agent (CSA), other than a chiral derivatizing agent (CDA). The absolute configurations of the pure enantiomers **1a** and **1b** were assigned to *S*- and *R*-configurations, respectively, based on NMR spectroscopic analysis with homochiral Phe-OMe as the chiral solvating agent. The assignments have been confirmed by single-crystal X-ray diffraction analysis. The present results suggest that this indirect CSA-NMR anisotropy methodology is applicable for the study of stereochemistry with certainty, not only restricted to the determination of enantiomeric purity.[27] Particularly for the host−guest complexes with multiple intermolecular interactions, the absolute stereochemistry can be assigned on the basis of the predictable anisotropic shielding effects caused by the specific alignment of a chiral solvating agent with an enantiomerically pure substrate.[28] In addition, the multiple intermolecular interactions between *S*-**1** and L-Phe-OMe are proved in the solid state by single-crystal X-ray diffraction analysis for the first time. The discussion in this article is helpful for the future applications of *R*- and *S*-**1** in chiral recognition and asymmetrical catalysis. Furthermore, the enantioselectivity of *R*- and *S*-**1** toward L/D-Phe-OMe and other chiral substrates is expected to be improved by structural modification to enhance the difference of steric repulsion or electron-donating/-accepting capacities between 5- and 15-*meso* sites. The investigation is currently underway in this laboratory.

EXPERIMENTAL SECTION

General Methods. Dichloromethane was freshly distilled from CaH_2 under nitrogen. Dipyrromethane,[29] *n*-hexadecyloxyl benzaldehyde,[30] and 2-methoxy-1-naphthylboronic acid[31] were prepared according to the published procedures. All other reagents and solvents were used as received. ^{1}H and ^{13}C NMR spectra were recorded on a 400 MHz NMR spectrometer in $CDCl_3$, and the chemical shifts were reported relative to internal $SiMe_4$. MALDI-TOF mass spectra were measured with dithranol as the matrix. Preparative chiral

dx.doi.org/10.1021/jo401825k | J. Org. Chem. 2013, 78, 9949−9955

high-performance liquid chromatography (HPLC) was performed at 20 °C and monitored by a UV detector at 410 nm.

X-ray Crystallography. Crystal data and details of data collection and structure refinement are given in Table 1. Data were collected at 150 K with a Mo Kα sealed tube (λ = 1.5418 Å) as light source, using a ω scan mode with an increment of 0.3°. Preliminary unit cell parameters were obtained from 45 frames. Final unit cell parameters were derived by global refinements of reflections obtained from integration of all the frame data. The collected frames were integrated using the preliminary cell-orientation matrix. The SMART software was used for collecting frames of data, indexing reflections, and determination of lattice constants;[32] SAINT-PLUS for the integration of intensity of reflections and scaling;[32] SADABS for absorption correction;[33] and SHELXL for space group and structure determination, refinements, graphics, and structure reporting.[34] CCDC-902733 and 949447 contain the supplementary crystallographic data for this paper. These data can be obtained free of charge from the Cambridge Crystallographic Data Centre via www.ccdc.cam.ac.uk/data_request/cif.

Synthesis of 5-Phenyl-15-(4-(hexadecyloxy)phenyl)-porphyrin (2). To a CH_2Cl_2 solution (100 mL) containing *n*-hexadecyloxyl benzaldehyde (346 mg, 1.00 mmol), benzaldehyde (106 mg, 1.00 mmol), and dipyrromethane (292 mg, 2.00 mmol) was added $BF_3{\cdot}Et_2O$ (0.02 mL, 0.16 mmol). The mixture was stirred for 15 h at room temperature under N_2 atmosphere. *p*-Chloranil (984 mg, 4.00 mmol) was added, and the mixture was stirred for 2 h. The solution containing the reaction mixture was concentrated and then chromatographed on an alumina column followed by a silica gel column with CH_2Cl_2 as the eluent, where the first fraction was collected and evaporated. The residue was chromatographed by an open GPC column with $CHCl_3$ as the eluent. The second fraction was collected and evaporated. Repeated chromatography followed by recrystallization from CH_2Cl_2 and methanol gave pure target compound as a dark purple powder (89.3 mg, 12.7%). ^{1}H NMR ($CDCl_3$, 400 MHz, 293 K): δ 10.341 (s, 2H), 9.424 (d, 4H, J = 4.8 Hz), 9.154 (d, 2H, J = 4.8 Hz), 9.109 (d, 2H, J = 4.8 Hz), 8.307 (m, 2H, J = 4.2 Hz), 8.205 (d, 2H, J = 8.4 Hz), 7.838 (t, 3H, J = 4.0 Hz), 7.368 (d, 2H, J = 8.4 Hz), 4.308 (t, 2H, J = 8.4 Hz), 2.038 (m, 2H), 1.678 (m, 2H), 1.308 (m, 24H), 0.912 (t, 3H, J = 8.0 Hz), −3.072 (s, 2H). ^{13}C NMR ($CDCl_3$, 100 MHz, 293 K): δ 159.1, 147.5, 147.2, 145.2, 141.4, 135.9, 134.9, 133.5, 131.5, 133.1, 131.0, 127.7, 127.0, 119.2, 118.9, 113.1, 105.2, 68.4, 32.0, 26.3, 22.7, 14.1. UV−vis ($CHCl_3$): λ_{max} (log ε) 409 (5.70), 504 (4.35), 539 (3.91), 576 (3.86), 632 nm (3.40). MALDI-TOF-MS: m/z calcd for $C_{48}H_{54}N_4O$ (M^+) 703.0, found 703.3. Anal. Calcd for $C_{48}H_{54}N_4O$: C, 82.01; H, 7.74; N, 7.97. Found: C, 81.79; H, 7.68; N, 7.83.

Synthesis of 5-Phenyl-15-(4-(hexadecyloxy)phenyl)-porphyrinatozinc Complex (3). To a $CHCl_3$/MeOH (2:1) solution (80 mL) containing **2** (140.8 mg, 0.20 mmol) was added a MeOH suspension of $Zn(OAc)_2{\cdot}2H_2O$ (350.4 mg, 0.40 mmol), and the reaction mixture was stirred for 12 h at room temperature. The solution containing the reaction mixture was concentrated and then chromatographed on a silica gel column with $CHCl_3$ as the eluent, where the second fraction was collected and evaporated. Repeated chromatography followed by recrystallization from $CHCl_3$ and methanol gave the pure target compound as a reddish purple powder (141 mg, 92.0%). ^{1}H NMR ($CDCl_3$, 400 MHz, 293 K): δ 10.307 (s, 2H), 9.432 (d, 4H J = 4.4 Hz), 9.158 (d, 2H, J = 4.4 Hz), 9.135 (d, 2H, J = 4.4 Hz), 8.263 (m, 2H), 8.160 (d, 2H, J = 8.4 Hz), 7.801 (m, 3H), 7.326 (d, 2H, J = 8.4 Hz), 4.290 (t, 2H, J = 8.0 Hz), 2.019 (m, 2H), 1.658 (m, 2H), 1.281 (m, 24H), 0.885 (d, 3H, J = 8.0 Hz). ^{13}C NMR ($CDCl_3$, 100 MHz, 293 K): δ 158.9, 150.5, 150.2, 149.5, 149.4, 142.7, 135.6, 134.6, 132.4, 131.7, 131.6, 126.6, 120.1, 119.9, 112.8, 106.1, 68.4, 31.9, 26.3, 22.7, 14.1. UV−vis ($CHCl_3$): λ_{max} (log ε) 409 (5.81), 536 (4.50), 573 nm (3.86). MALDI-TOF-MS: m/z calcd for $C_{48}H_{52}N_4OZn$ (M^+) 766.3, found 765.7. Anal. Calcd for $C_{48}H_{52}N_4OZn$: C, 75.23; H, 6.84; N, 7.31. Found: C, 74.86; H, 6.79; N, 7.18.

Synthesis of 5-Bromo-10-phenyl-20-(4-(hexadecyloxy)-phenyl)porphyrinatozinc Complex (4). NBS (18.2 mg, 1.1 equiv) and pyridine (0.1 mL) were added to a solution of **3** (76.6 mg, 0.1 mmol) in degassed $CHCl_3$ (20 mL), and the mixture was stirred for 10 min under a N_2 atmosphere at 0 °C in the dark. The solvent was evaporated and the residue was subjected to chromatography on a silica-gel column with CH_2Cl_2/ Hexane (1:2, v/v) as the eluent. Repeated chromatography followed by recrystallization from $CHCl_3$ and methanol gave pure target compound as reddish purple crystals (25.6 mg, 30.3%). ^{1}H NMR ($CDCl_3$, 400 MHz, 293 K): δ 10.249 (s, 1H), 9.836 (m, 2H, J = 2.4 Hz), 9.391 (t, 2H, J = 4.8 Hz), 9.126 (t, 2H, J = 4.8 Hz), 9.065 (t, 2H, J = 2.4 Hz), 8.243 (m, 2H), 8.139 (d, 2H, J = 8.4 Hz), 7.821 (m, 3H), 7.338(d, 2H, J = 8.8 Hz), 4.310 (t, 2H, J = 4.0 Hz), 2.039 (m, 2H), 1.668 (m, 2H), 1.301 (m, 24H), 0.905 (t, 3H, J = 4.0 Hz); ^{13}C NMR ($CDCl_3$, 100 MHz, 293 K): δ 159.0, 150.9, 150.8, 150.6, 150.4, 150.1, 149.2, 142.3, 135.6, 134.5, 133.2, 133.0, 132.8, 132.7, 132.0, 131.9, 127.6, 126.7, 121.2, 120.9, 112.8, 106.4, 104.9, 68.4, 32.0, 26.3, 22.7, 14.1; UV-*vis* ($CHCl_3$): λ_{max} (log ε) 409 (5.81), 536 (4.50), 573 (3.86). MALDI-TOF-MS: m/z calcd for $C_{48}H_{51}BrN_4OZn$ (M^+) 845.2, found 845.4. Anal. Calcd for $C_{48}H_{51}BrN_4OZn$: C, 68.21; H, 6.08; N, 6.63. Found: C, 68.55; H, 6.18; N, 6.75.

Synthesis of 5-Phenyl-10-(2-methoxynaphthyl)-15-(4-(hexadecyloxy)phenyl)porphyrinatozinc Complex (5). To a solution containing compound **4** (42.3 mg, 0.05 mmol) in DMF (1 mL) and toluene (1 mL) were added K_2CO_3 (55.2 mg, 0.40 mmol), $Pd(PPh_3)_4$ (21.50 mg, 0.015 mmol), and 2-methoxy-1-naphthylboronic acid (25.25 mg, 0.125 mmol). The resulting reaction mixture was refluxed for 20 h under N_2 and then cooled to room temperature. The volatiles were removed under reduced pressure. The residue was chromatographed on a silica gel column (CH_2Cl_2/hexane = 1:1), where the second fraction was collected and evaporated to give **5** as a reddish purple powder (32.2 mg, 69.8%). ^{1}H NMR ($CDCl_3$, 400 MHz, 293 K): δ 10.246 (s, 1H), 9.392 (d, 2H, J = 4.4 Hz), 9.126 (d, 2H, J = 4.4 Hz), 9.075 (d, 2H, J = 4.4 Hz), 8.931 (d, 2H, J = 4.8 Hz), 8.684 (d, 2H, J = 4.0 Hz), 8.328 (d, 1H, J = 8.2 Hz), 8.228 (m, 2H), 8.123 (t, 2H, J = 3.4 Hz), 8.059 (d, 1H, J = 8.0 Hz), 7.745 (m, 4H), 7.315 (d, 2H, J = 4.0 Hz), 6.941 (t, 1H, J = 8.2 Hz), 6.761 (d, 1H, J = 8.4 Hz), 4.245 (t, 2H, J = 8.8 Hz), 3.654 (s, 3H), 1.981 (m, 2H), 1.624 (m, 2H), 1.506 (m, 2H), 1.271 (m, 22H), 0.878 (t, 3H, J = 8.4 Hz). ^{13}C NMR ($CDCl_3$, 100 MHz, 293 K): δ 158.8, 157.5, 150.7, 150.6, 150.5, 150.2, 150.1, 149.6, 142.8, 135.5, 134.6, 134.5, 132.4, 131.5, 131.4, 130.3, 128.5, 127.5, 126.6, 126.5, 123.4, 120.1, 113.6, 112.7, 112.6, 106.0, 68.4, 56.9, 32.0, 29.8, 26.3, 22.7, 14.2; UV−vis ($CHCl_3$): λ_{max} (log ε) 416 (5.73), 542 (4.44), 579 nm (3.66). MALDI-TOF-MS: m/z calcd for $C_{59}H_{60}N_4O_2Zn$ (M^+) 922.5, found 922.2. Anal. Calcd for $C_{59}H_{60}N_4O_2Zn$: C, 76.81; H, 6.56; N, 6.07. Found: C, 77.09; H, 6.69; N, 6.15.

Synthesis of 5-Phenyl-10-(2-hydroxynaphthyl)-15-(4-hydroxyphenyl)porphyrin (6). A 100 mL round bottomed flask with a reflux condenser was charged with **5** (36.84 mg, 0.04 mmol) in CH_2Cl_2 (10 mL). A 1.0 M BBr_3 solution in CH_2Cl_2 (1.0 mL) was added dropwise at 0 °C. After the solution was stirred at room temperature for 1.5 h, water (10 mL) was added to the reaction mixture, and the organic layer was washed with saturated $NaHCO_3$ (aq) (3 × 100 mL) and water (3 × 100 mL) and dried over Na_2SO_4. After evaporation, **6** were obtained as a purple powder (18.36 mg, 80%). ^{1}H NMR ($CDCl_3$, 400 MHz, 293 K): δ 10.291 (s, 1H), 9.370 (d, 2H, J = 7.6 Hz), 9.040 (t, 2H J = 4.8 Hz), 8.861 (t, 2H, J = 6.8 Hz), 8.684 (d, 2H, J = 4.8 Hz), 8.235 (m, 3H), 8.044 (m, 3H), 7.760 (m, 3H), 7.640 (d, 2H, J = 9.2 Hz), 7.326 (t, 1H, J = 8.4 Hz), 7.254(s, 2H), 7.120 (m, 2H), 6.993 (t, 1H, J = 8.4 Hz), 6.798 (d, 1H, J = 8.4 Hz), 5.08 (br, 2H), −2.854 (s, 2H). ^{13}C NMR ($CDCl_3$, 100 MHz, 293 K): δ 155.2, 154.3, 141.4, 137.8, 135.9, 135.8, 134.7, 134.6, 133.9, 132.0, 131.6, 130.9, 128.5, 127.8, 127.7, 126.9, 126.9, 126.9, 121.2, 119.8, 119.7, 117.4, 113.9, 109.0, 106.0. UV−vis ($CHCl_3$): λ_{max} (log ε) 415 (5.60), 510 (4.37), 545 (3.79), 583 (3.89), 637 nm (3.40). MALDI-TOF-MS: m/z calcd for $C_{42}H_{28}N_4O_2$ (M^+) 620.7, found 621.9. Anal. Calcd for $C_{42}H_{28}N_4O_2{\cdot}CH_3OH$: C, 79.12; H, 4.94; N, 8.58. Found: C, 79.18; H, 4.67; N, 8.55.

Synthesis of 5-Phenyl-10-(2-hydroxynaphthyl)-15-(4-hydroxyphenyl)porphyrinatozinc Complex (1). To a $CHCl_3$/MeOH (2:1) solution (20 mL) containing **6** (46.1 mg, 0.05 mmol) was added a MeOH suspension of $Zn(OAc)_2{\cdot}2H_2O$ (235.0 mg, 0.40 mmol), and the reaction mixture was stirred for 12 h at room temperature. The solution containing the reaction mixture was concentrated and then chromatographed on a silica gel column with $CHCl_3$ as a eluent, where the second fraction was collected and evaporated. Repeated

dx.doi.org/10.1021/jo401825k | J. Org. Chem. 2013, 78, 9949−9955

chromatography followed by recrystallization from $CHCl_3$ and methanol gave pure target compound as a reddish purple powder (31.5 mg, 92.0%). ^{1}H NMR ($CDCl_3$, 400 MHz, 293 K): δ 10.352 (s, 1H), 9.462 (d, 2H, J = 4.8 Hz), 9.151 (d, 2H, J = 4.8 Hz), 8.972 (d, 2H, J = 4.6 Hz), 8.784 (d, 2H, J = 4.8 Hz), 8.265 (m, 3H), 8.096 (t, 3H, J = 8.8 Hz), 7.792 (t, 3H, J = 8.6 Hz), 7.661 (d, 1H, J = 8.4 Hz), 7.348 (m, 1H), 7.211 (d, 2H, J = 8.6 Hz), 7.000 (t, 1H, J = 8.6 Hz), 6.776 (d, 1H, J = 8.4 Hz), 5.25 (s, 1H), 5.09 (s, 1H); ^{13}C NMR ($CDCl_3$, 100 MHz, 293 K): δ 154.1, 150.9, 150.8, 150.7, 150.5, 149.8, 142.4, 135.7, 134.6, 133.2, 132.8, 132.1, 132.0, 131.2, 131.1, 130.6, 128.5, 127.7, 127.6, 126.9, 126.6, 126.5, 123.2, 117.3, 113.6, 107.0; UV−vis ($CHCl_3$): λ_{max} (log ε) 415 (5.76), 541 nm (4.67). MALDI-TOF-MS m/z calcd for $C_{42}H_{26}N_4O_2Zn$ (M^+) 684.1, found 683.3. Anal. Calcd for $C_{42}H_{26}N_4O_2Zn{\cdot}2CH_3OH$: C, 70.63; H, 4.58; N, 7.49. Found: C, 70.00; H, 4.19; N, 7.87.

■ ASSOCIATED CONTENT

Supporting Information

^{1}H NMR and ^{13}C NMR spectra of all new compounds. Crystallographic data for **1** and **1a**·L-Phe-OMe. Method for evaluation of association constants (K_{assoc}); ^{1}H NMR spectra of L-Phen-OMe, **1a**·L-Phe-OMe, **1b**·L-Phe-OMe, **1a**·D-Phe-OMe and **1b**·D-Phe-OMe; ^{1}H−^{1}H COSY and ^{1}H−^{1}H NOESY spectra of **1a**·L-Phe-OMe, **1b**·L-Phe-OMe. Density functional theory calculations. ^{1}H NMR titration of **1a** and **1b** with L-Phen-OMe. CIF files of **1** and **1a**·L-Phe-OMe. This material is available free of charge via the Internet at http://pubs.acs.org.

■ AUTHOR INFORMATION

Corresponding Author

*E-mail: yzbian@ustb.edu.cn.

Notes

The authors declare no competing financial interest.

■ ACKNOWLEDGMENTS

Financial support from the Natural Science Foundation of China, National Ministry of Science and Technology of China (Grant No. 2012CB224801), Program for New Century Excellent Talents in University, Fundamental Research Funds for the Central Universities, and Beijing Natural Science Foundation is gratefully acknowledged.

■ REFERENCES

(1) Hembury, G. A.; Borovkov, V. V.; Inoue, Y. *Chem. Rev.* **2008**, *108*, 1−73.
(2) Xu, X.; Lu, H.; Ruppel, J. V.; Cui, X.; de Mesa, S. L.; Wojtas, L.; Zhang, X. P. *J. Am. Chem. Soc.* **2011**, *133*, 15292−15295.
(3) Huang, X.; Nakanishi, K.; Berova, N. *Chirality* **2000**, *12*, 237−255.
(4) Marchon, J.-C.; Ramasseul, R. In *The Porphyrin Handbook*; Kadish, K. M., Smith, K. M., Guilard, R., Eds.; Academic Press: Amsterdam, 2003; Vol. *11*, pp 75−132.
(5) Ferrand, Y.; Le Maux, P.; Simonneaux, G. *Org. Lett.* **2004**, *6*, 3211−3214.
(6) Ogoshi, H.; Mizutani, T. *Acc. Chem. Res.* **1998**, *31*, 81−89.
(7) Konishi, K.; Takahata, Y.; Aida, T.; Inoue, S. *J. Am. Chem. Soc.* **1993**, *115*, 1169−1170.
(8) Lindsey, J. S. *Acc. Chem. Res.* **2010**, *43*, 300−311.
(9) Mizutani, T.; Ema, T.; Tomita, T.; Kuroda, Y.; Ogoshi, H. *J. Am. Chem. Soc.* **1994**, *116*, 4240−4250.
(10) Ogoshi, H.; Saita, K.; Watanabe, T.; Toi, H.; Aoyama, Y. *Tetrahedron Lett.* **1986**, *27*, 6365−6368.
(11) Mizutani, T.; Kurahashi, T.; Murakami, T.; Matsumi, N.; Ogoshi, H. *J. Am. Chem. Soc.* **1997**, *119*, 8991−9001.
(12) Egorova, O. A.; Tsay, O. G.; Khatua, S.; Huh, O. J.; Churchill, D. G. *Inorg. Chem.* **2009**, *48*, 4634−4636.
(13) Wallace, D. M.; Leung, S. H.; Senge, M. O.; Smith, K. M. *J. Org. Chem.* **1993**, *58*, 7245−7257.
(14) Senge, M. O.; Shaker, Y. M.; Pintea, M.; Ryppa, C.; Hatscher, S. S.; Ryan, A.; Sergeeva, Y. *Eur. J. Org. Chem.* **2010**, 237−258.
(15) Hayashi, T.; Miyahara, T.; Hashizume, N.; Ogoshi, H. *J. Am. Chem. Soc.* **1993**, *115*, 2049−2051.
(16) Adams, H.; Chekmeneva, E.; Hunter, C. A.; Misuraca, M. C.; Navarro, C.; Turega, S. M. *J. Am. Chem. Soc.* **2013**, *135*, 1853−1863.
(17) Senge, M. O. *Chem. Commun.* **2011**, *47*, 1943−1960.
(18) Gao, Y.; Zhang, X.; Ma, C.; Li, X.; Jiang, J. *J. Am. Chem. Soc.* **2008**, *130*, 17044−17052.
(19) Suzuki, A. *Angew. Chem., Int. Ed.* **2011**, *50*, 6722−6737.
(20) Senge, M. O. *In The Porphyrin Handbook*; Kadish, K. M., Smith, K. M., Guilard, R., Eds.; Academic Press: San Diego, CA, 2000; Vol. *10*, p 8.
(21) Wu, X.; Starnes, S. D. *Org. Lett.* **2012**, *14*, 3652−3655.
(22) Shoji, Y.; Tashiro, K.; Aida, T. *J. Am. Chem. Soc.* **2010**, *132*, 5928−5929.
(23) Kuroda, Y.; kato, Y.; Higashioji, T.; Hasegawa, J.; Kawanami, S.; Takahashi, M.; Shiraishi, N.; Tanabe, K.; Ogoshi, H. *J. Am. Chem. Soc.* **1995**, *117*, 10950−10958.
(24) Chai, J. D.; Head-Gordon, M. *Phys. Chem. Chem. Phys.* **2008**, *10*, 6615−6620.
(25) Huang, X.; Fujioka, N.; Pescitelli, G.; Koehn, F. E.; Williamson, R. T.; Nakanishi, K.; Berova, N. *J. Am. Chem. Soc.* **2002**, *124*, 10320−10335.
(26) Wagging of the ester group around the C*−COOMe bond is faster than the NMR time scale in the present case, which may lead to the shielding of pyrrole protons on both sides.
(27) Seco, J. M.; Quiñoá, E.; Riguera, R. *Chem. Rev.* **2012**, *112*, 4603−4641.
(28) Wenzel, T. J.; Chisholm, C. D. *Chirality* **2011**, *23*, 190−214.
(29) Laha, J. K.; Dhanalekshmi, S.; Taniguchi, M.; Ambroise, A.; Lindsey, J. S. *Org. Process Res. Dev.* **2003**, *7*, 799−812.
(30) Nakanishi, T.; Miyashita, N.; Michinobu, T.; Wakayama, Y.; Tsuruoka, T.; Ariga, K.; Kurth, D. G. *J. Am. Chem. Soc.* **2006**, *128*, 6328−6329.
(31) Markov, A. V.; Ramírez-López, P.; Biedermannová, L.; Rulíšek, L.; Dufková, L.; Kotora, M.; Zhu, F. J.; Kočovský, P. *J. Am. Chem. Soc.* **2008**, *130*, 5341−5348.
(32) SMART and SAINT for Windows NT Software Reference Manuals, Version 5.0, Bruker Analytical X-Ray Systems, Madison, WI, 1997.
(33) Sheldrick, G. M. SADABS, A Software for Empirical Absorption Correction; University of Göttingen: Göttingen, Germany, 1997.
(34) SHELXL Reference Manual, version 5.1; Bruker Analytical X-Ray Systems: Madison, WI, 1997.